04.1;06.4

Obtaining glass ceramics of the $MgO-SiO_2$ system by the plasma melting method

© V.V. Shekhovtsov[1], O.G. Volokitin[1], V.A. Ushakov[2], D.A. Zorin[2]

[1] Tomsk state university of architecture and building, Tomsk, Russia
[2] Moscow State University of Civil Engineering, Moscow, Russia
E-mail: shehovcov2010@yandex.ru

Received June 10, 2022
Revised October 12, 2022
Accepted October 21, 2022

Results of experimental studies of the synthesis of glass ceramics of the $MgO-SiO_2$ system by plasma melting at the atmospheric pressure are presented. Electron microscopy data showed that, during the melt crystallization with the rate of 287−5 K/s, the surface morphology is represented by a dense packing of rhombic dodecahedral Mg_2SiO_4 crystals (without open porosity). In this case, the matrix is characterized by the formation of a dense framework with a clear linear arrangement of spherical inclusions corresponding to the $MgSiO_3$ phase. As a result of the plasma melting synthesis, glass ceramics with the density of 3.56 g/cm^3 and microhardness of up to 15 GPa was obtained. It is assumed that glass ceramics with such a composition can be considered as an excellent option for the development of a cost-effective high-quality refractory.

Keywords: forsterite, glass ceramics, electric arc synthesis.

DOI: 10.21883/TPL.2022.12.54948.19278

Synthesis of glass-ceramic materials of the $MgO-SiO_2$ system is a topical issue in view of a wide range of their application in many high-tech production processes [1–3]. This system includes two binary compounds: magnesium orthosilicate Mg_4SiO_2 (forsterite) and magnesium metasilicate $MgSiO_3$ existing in three polymorphic modifications (enstatite, clinoenstatite, and protoenstatite [4]). Due to the absence of polymorphic transformations in the forsterite phase, ceramic materials based on it are not susceptible to aging, which meets the requirements of the state−of−the−art material science. However, experimental investigation is fraught with difficulties associated with the high melting temperature (2160 ± 30 K). At the stage of discussing the investigation topicality, it is necessary to notice that formation of the $MgO-SiO_2$ system phases is important also for such a field as geophysics that studies the Earthś mantle processes [5,6]. An alternative method for the heat energy generation is based on using the electric arc plasma [7,8]. The source of this type allows realizing high specific heat fluxes, which provides high temperatures of fluxes impinging on solid-state raw materials (mass-average temperature $T \sim 5000$ K). The main tasks of developing the method of exposing various-category materials to plasma are optimizing the process flow chart and facilities, searching for potential fields of efficient application, and obtaining competitive materials. As a possible solution, there may be the use of intense specific heat fluxes formed by a thermal plasma jet in the process of obtaining the melt from refractory raw materials of the $MgO-SiO_2$ group and its crystallization under the condition of intense heat exchange in the environment. This paper presents the results of experiments devoted to obtaining glass ceramics of the $MgO-SiO_2$ system from a melt of common natural raw materials (magnesite $MgCO_3$, quartz sand SiO_2) obtained in the medium of the atmospheric-pressure thermal plasma. Notice that we have not found any references on possible implementation of such a method of obtaining glass-ceramic materials.

In the course of a series of experimental investigations, at the first stage there was performed an isothermal exposure of magnesite at 1273 K for 3 h in order to decompose $MgCO_3$ into MgO and CO_2. The selected mode of the magnesite thermal decomposition was established based on the results of studies involving the differential thermal analysis (NETZSCH STA 409 PC/PG) which have shown that in the temperature range of 853 to 1009 K there takes place the $MgCO_3$ dissociation characterized by two intense endothermal peaks. Overall endothermic reactions are characterized by the following parameters: area of 1457 J/g, height of 3.26 mW/mg. Loss of mass is 50.9%. The obtained data are consistent with the results of thermal treatment of magnesian materials [9]. Similar investigations on quartz sand SiO_2 showed that in the temperature interval of 843.1 to 853.7 K an endothermal peak is observed whose area is 13.16 J/g and height is 0.1913 mW/mg. Due to removal of isomorphic impurities and gas−liquid inclusions, the mass loss does not exceed 1%. At the second stage, the materials were mixed in the stoichiometric ratio $MgO/SiO_2 \sim 1.34$, which complies with the theoretical composition of forsterite ceramics Mg_2SiO_4. The prepared stock was ground in a planetary ball mill to the fraction below 71 μm. The obtained powder was granulated using a testing sieve with the cell of 2 mm so as to prevent its blowing out of the plasma−affected area. As a binding

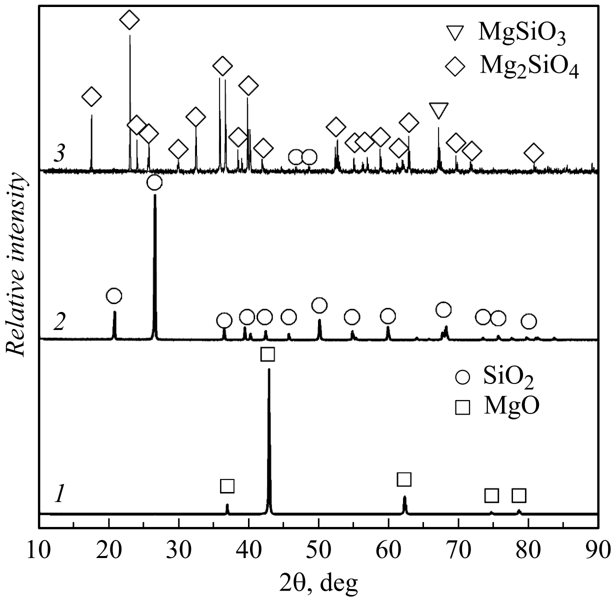

Figure 1. Typical X−ray diffraction patterns of the products of isothermal reactions of magnesite MgO (*1*) and quartz sand SiO$_2$ (*2*), and of the product of the electric-arc plasma synthesis at the stoichiometric ratio MgO/SiO$_2$ ~ 1.34 (*3*).

agent, we used polyvinyl alcohol 6/1 that is typically used in forming powders for ceramics. A portion of the obtained agglomerated powder 7 g in weight was put into a graphite crucible (anode); after that, the electric-arc plasmatron (cathode) was started. The experimental parameters were as follows: current of 100 A, voltage of 120 V, plasma-forming gas (air) consumption of 12 l/min, melting time of 30 s. In the course of the experiments, temperature of the graphite crucible outer wall was fixed by infrared thermometry (pyrometer GM 2200, measurement range of 200−2200°C). At the specified parameters, temperature of the graphite crucible outer wall remained equal to 2320 ± 20 K during 30 s; the rate of the crucible cooling after the end of exposure to the plasma arc was 287 ± 5 K/s. At the given experimental parameters, the process output products are semi-spherical samples with the following characteristics: diameter/thickness ratio of 25/12 mm, mass of 6.5 ± 0.3 g, bulk density of 3.35 g/cm. The obtained samples were examined by the methods of X−ray diffractometry based on CuK_α radiation with the scanning rate of 2 deg/min in the range $2\theta = 10{-}90$ deg (Shimadzu XRD 6000, Japan) and scanning electron microscopy with energy−dispersion analysis (Quanta 200 3D, USA). Hardness of the glass-ceramic samples was measured with the microhardness tester PMT3 (with the loading mass of 500 g by Vickers test).

The X−ray diffractometry data shows that the initial materials (Fig. 1, curves *1* and *2*) are represented by the MgO and SiO$_2$ modifications; their crystallinities are 97 and 98%, respectively. The established phases comply with the known data on typical phase compositions of the materials used in [10]. The diffraction pattern of the synthesized sample with the stoichiometric ratio MgO/SiO$_2$ ~ 1.34 (Fig. 1, curve *3*) demonstrates that the material matrix consists of forsterite Mg$_2$SiO$_4$ ($a = 1.824$ nm, $b = 0.884$ nm, $c = 0.519$ nm, orthorhombic syngony) and high-temperature modification of clinoenstatite MgSiO$_3$ ($a = 0.476$ nm, $b = 1.022$ nm, $c = 0.599$ nm, orthorhombic syngony). At the same time, there is a low-intense peak at about 44−47.5 deg which corresponds to the silicon dioxide modification, namely, cristobalite SiO$_2$ ($a = 0.711$ nm, $b = 0.702$ nm, $c = 0.698$ nm, tetragonal syngony). The glass phase content does not exceed 12 wt.%.

The morphology of particles of the initial magnesite and quartz sand (Fig. 2, *a*) is represented by a laminated structure of densely structured prismatic agglomerates. The energy-dispersion analysis in the spectrum region of $130 \times 100\,\mu$m showed that the predominant components of magnesite are O and Mg, while that of quartz sand is Si; in addition, there are Al, Ca, and Fe in the amounts of units and fractions of percent (Fig. 2, *d*). As per the scanning electron microscopy data, the surface of the synthesized ceramic sample exhibits a dense packing of rhombic dodecahedral crystals with the following sizes: $a = 240 \pm 10\,\mu$m, $b = 180 \pm 20\,\mu$m (Fig. 2, *b*). According to the data of energy-dispersion analysis of the crystal surface (spectrum region $80 \times 75\,\mu$m), the elemental composition is Mg ~ 32.49 wt.%, Si ~ 29.23 wt.%, which is characteristic of the Mg$_2$SiO$_4$ phase (Fig. 2, *d*). The obtained electronic images (Fig. 2, *c*) of the surface of the synthesized sample cleave evidence for the formation of a dense framework with a clear linear arrangement of spherical inclusions, each of them having a scar in the center.

The energy-dispersion spectrum of the spherical inclusion surface demonstrates the predominance of Si ~ 34.19 wt.% above Mg ~ 17.04 wt.%, which is characteristic of the MgSiO$_3$ composition (Fig. 2, *d*). The elemental composition of the phase uniformly embracing those inclusions is Si ~ 22.68 wt.%, Mg ~ 32.29 wt.%, which is typical of Mg$_2$SiO$_4$. In both cases, impurities Al, Ca, and Fe are present, whose concentration does not exceed 2 wt.%, which is caused by the initial content of the used materials. The absence of impurities on the surface is achieved due to an intense influence of the heat flux from plasma, which induces overheating and partial evaporation of the impurities.

Thus, the following aspect of physical process has been defined for the formation of MgO−SiO$_2$ ceramic samples with the stoichiometric ratio MgO/SiO$_2$ ~ 1.34 from the melt obtained with the assistance of thermal plasma: melting in the thermal plasma medium is an incongruent process, the Mg$_2$SiO$_4$ formation center is the SiO$_2$ phase. Mg^{2+} ions diffuse into the SiO$_2$ surface due to the difference in viscous forces ($\eta_{\mathrm{SiO_2}} = 10^6\,\mathrm{Pa\cdot s}$, $\eta_{\mathrm{MgO}} = 0.0573\,\mathrm{Pa\cdot s}$ at the melting point), thus forming the MgSiO$_3$ initial phase. Then, after the boundary layer (Mg$_2$SiO$_4$ $\to$ MgSiO$_3$ $\to$ SiO$_2$) gets overheated, the heat transfer induces formation of

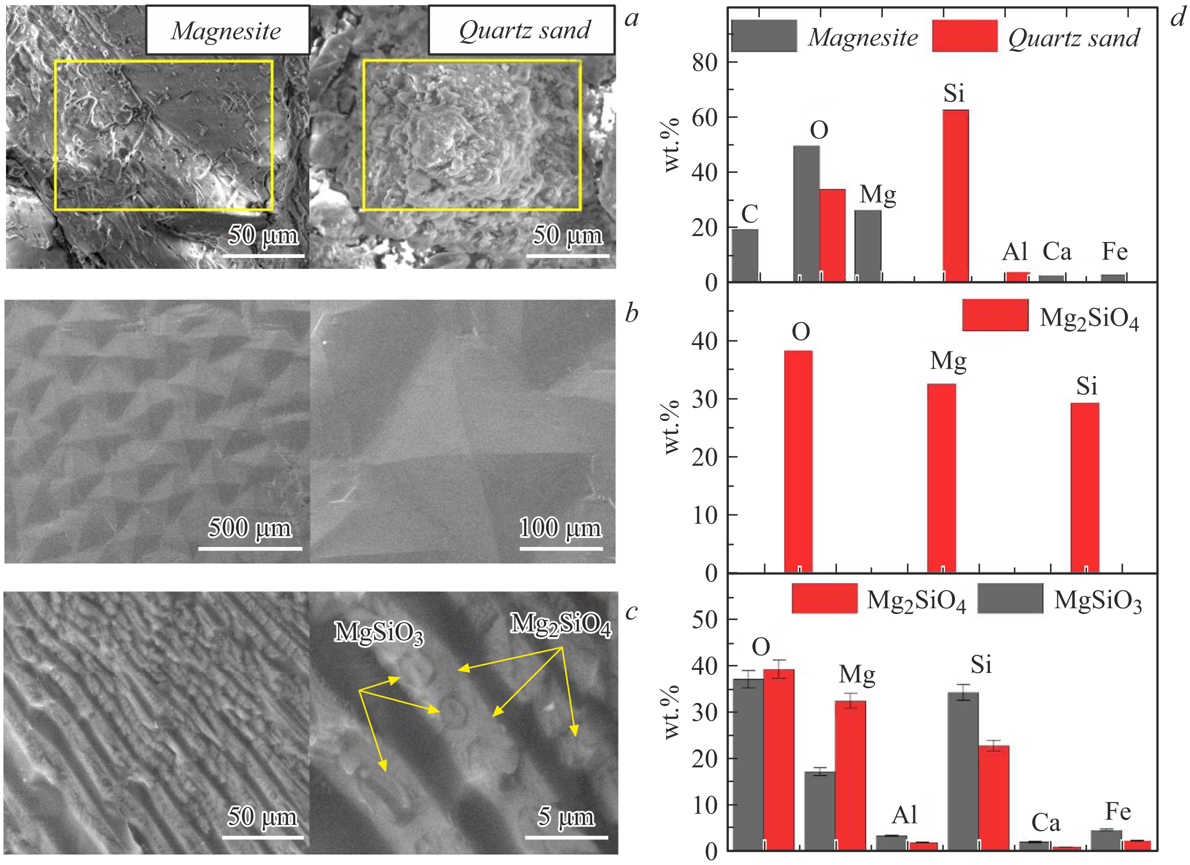

Figure 2. Results of the scanning electron microscopy and energy-dispersion analysis. *a* — photo of surfaces of the initial material particles, *b* — photo of the surface of the synthesized ceramic sample, *c* — photo of the surface of the synthesized ceramic sample cleave, *d* — relevant energy-dispersion spectra.

a front of polymorphic transformations whose vector is directed towards the SiO_2 center. As the major amount of Mg^{2+} passes through the SiO_2 surface and gets into its core, the reaction of the Mg_2SiO_4 phase formation proceeds on the side of the $MgSiO_3$ surface layer due to the increase in the Mg potential in the melt. At the same time, formation of new $MgSiO_3$ proceeds in the direction towards the SiO_2 core. Finally, SiO_2 completely passes into the $MgSiO_3$ phase due to continuous diffusion in the liquid phase.

Microhardness analysis of a section of the synthesized glass-ceramic sample showed that the highest hardness was 15.0 ± 0.2 GPa, while the value averaged over a series of measurements was 13.2 GPa. Such hardness values comply with the glass-ceramic samples based on the $MgO-SiO_2$ system which were obtained by other techniques [11]. Hence, the obtained material is competitive and may be regarded as an excellent option for developing one of the high-quality low-cost refractories.

The conducted experiments demonstrated the possibility of synthesizing glass ceramics of the $MgO-SiO_2$ system from magnesite and quartz sand by plasma-assisted melting. Electron microscopy data showed that, during the melt crystallization with the rate of 287–5 K/s, the surface morphology is represented by a dense packing of rhombic–dodecahedral Mg_2SiO_4 crystals (without open porosity). The matrix is thereat characterized by the existence of a dense framework with a clear linear arrangement of spherical inclusions corresponding to the $MgSiO_3$ phase. As a result, the plasma-assisted melting method provided glass ceramics with the density of 3.56 g/cm^3 and microhardness of up to 15 GPa. The obtained results are of interest in view of developing techniques for synthesizing glass-ceramic materials.

Acknowledgements

The study was performed by using facilities of the Tomsk Material–Science CCU belonging to the Tomsk Regional CCU of the Tomsk State University.

Financial support

The study was financially supported by the MSCEU Research and Development Administration in the framework of a tender (2022) for conducting fundamental and applied researches (R&D/R&AD) by research teams of institutions–members of the Branch Consortium „Civil Engineering and Architecture“ (Contract № 6/K of 27.05.2022) for the purpose of executing the MSCEU RDA development program for 2021–2030 in the scope of realizing the Program of Strategic Academic Leadership „Priority-2030".

Conflict of interests

The authors declare that they have no conflict of interests.

References

[1] S.P. Sahoo, S. Pradhan, J. Mukherjee, V.S. Rawat, Opt. Laser Technol., **151**, 108050 (2022). DOI: 10.1016/j.optlastec.2022.108050
[2] Y. Huh, K.J. Hong, M.S. Han, S. Kang, Thin Solid Films, **752**, 139258 (2022). DOI: 10.1016/j.tsf.2022.139258
[3] M. Nguyen, R. Sokolář, Materials, **15** (4), 1363 (2022). DOI: 10.3390/ma15041363
[4] T. Gasparik, in *Phase diagrams for geoscientists* (Springer, Berlin–Heidelberg, 2003), p. 13–31. DOI: 10.1007/978-3-540-38352-9_2
[5] N.G. Rudraswami, M.D. Suttle, Y. Marrocchi, S. Taylor, J. Villeneuve, Geochim. Cosmochim. Acta, **325**, 1 (2022). DOI: 10.1016/j.gca.2022.03.015
[6] I.B. Agama, G. Chazot, P. Kamgang, Acta Geochim., **41** (1), 12 (2022). DOI: 10.1007/s11631-021-00513-y
[7] A.Ya. Pak, V.E. Gubin, G.Ya. Mamontov, Tech. Phys. Lett., **46** (7), 695 (2020). DOI: 10.1134/S1063785020070226.
[8] V.V. Shekhovshov, O.G. Volokitin, O.V. Matvienko, Russ. Phys. J., **64**, 1443 (2021). DOI: 10.1007/s11182-021-02477-1.
[9] N.A. Mitina, V.A. Lotov, Refract. Industr. Ceram., **58** (3), 331 (2017). DOI: 10.1007/s11148-017-0105-0.
[10] U. Nurbaiti, T. Darminto, M. Zainuri, S. Pratapa, Ceram. Int., **44** (5), 5543 (2018). DOI: 10.1016/j.ceramint.2017.12.198
[11] G.A. Khater, E.M. Safwat, J. Non-Cryst. Solids, **563**, 120810 (2021).